# Logarithmic Term in the Density Expansion of Transport Coefficients*

K. KAWASAKI AND I. OPPENHEIM
*Department of Chemistry, Massachusetts Institute of Technology, Cambridge, Massachusetts*
(Received 29 April 1965)

A divergence in the first (second) density correction to the transport coefficients of two- (three-) dimensional classical gases has been studied using the resolvent-operator formalism of the correlation-function expressions for the transport coefficients. As an illustration we consider the self-diffusion coefficient of the two-dimensional gas. A divergence in the triple-collision term arises from the behavior of the integrand at small values of the wave vector in the integration over the wave vector. Similar and stronger divergences appear in higher terms of the binary-collision expansion. The most divergent terms have been summed with the help of a diagram analysis and are shown to provide a natural cutoff to the divergence in the triple-collision term. The cutoff wave vector is proportional to the density $\rho$ and gives rise to a term involving $\ln\rho$ in the density correction to the transport coefficients.

## 1. INTRODUCTION

RECENTLY, Cohen, Dorfman, and Sengers[1] discovered that the triple-(quadruple-) collision terms which appear in the first (second) density correction to the transport coefficients in two- (three-) dimensional classical gases interacting with short-range repulsive forces contain certain divergences arising from the fact that the contributing phase-space regions can become indefinitely large in the neighborhood of certain well-collimated collisions. They suggested that the transport coefficients ($\eta$, the viscosity coefficient, $\kappa$, the thermal conductivity; and $\rho D$, where $D$ is the diffusion constant) of gases might not be analytic functions of the density $\rho$ near $\rho=0$, and that the density expansion might involve $\ln\rho$ besides powers of $\rho$. This indicates that some of the basic assumptions in the transport theory of dense gases, notably Bogolyubov's functional assumption,[2] break down at a certain stage of the density expansion. This has already been anticipated by Green[3] from the slow time decay of the error term which expresses the deviation from Bogolyubov's functional assumption.

A somewhat different method for obtaining density expansions of the transport coefficients has been developed by Zwanzig[4] and the present authors[5] starting from the correlation-function formulas for the transport coefficients which are expressed in terms of the $N$-body resolvent operator. We make use of the binary-collision expansion of this $N$-body resolvent operator, and invert the resulting series for the reduced one- or two-body resolvent operators. We do not use a statistical or functional assumption similar to that mentioned in the preceding paragraph. Instead, our basic assumption has been that the inverted series gives a well-defined expansion of the transport coefficients in powers of the density. This has been verified up to the first density correction in the three-dimensional gas interacting with short-range forces.

The discovery of the divergence necessitates a re-examination of our method; the main object of the present work is to present the results of this re-examination. We consider as an illustration the self-diffusion coefficient of the two-dimensional gas. In Sec. 2 we give a formal expression for the self-diffusion constant up to the first density correction which involves the triple-collision operator and we classify various terms (diagrams) contributing to the density correction. In Sec. 3 we express the triple collision term in the $\mathbf{k}$ representation and demonstrate that in two dimensions a logarithmic divergence arises in the $\mathbf{k}$ integration from the neighborhood of $\mathbf{k}=0$. We also find that stronger divergences appear in higher terms of the binary-collision expansion. With the help of diagrams we sum over the most divergent contributions (ring diagrams) in each power of $\rho$, and demonstrate that the sum provides a natural cutoff to the logarithmic divergences in the triple-collision term, producing a $\ln\rho$ term in the self-diffusion coefficient. The last section is devoted to a brief summary and remarks concerning other transport coefficients and three-dimensional gases.

## 2. SELF-DIFFUSION COEFFICIENT

For illustration purposes, we consider the self-diffusion coefficient $\mathbf{D}$ of a system consisting of $N$ monatomic classical particles of mass $m$ which interact with two-body short-range repulsive forces. The correlation function expression for $\mathbf{D}$ is

$$\mathbf{D}\equiv\lim_{\epsilon\to 0+}(1/m^2)\langle p_1{}^x G(\epsilon) p_1{}^x\rangle, \tag{2.1}$$

where $p_1{}^x$ is the $x$ component of the momentum of particle 1, $G(\epsilon)$ is the resolvent operator defined in I and $\langle\cdots\rangle$ denotes an average over the equilibrium ensemble.[4]

* Work supported by the National Science Foundation and the U. S. Air Force Cambridge Research Laboratories.

[1] E. G. D. Cohen and R. Dorfman, Phys. Letters **16**, 124 (1965), and J. V. Sengers (private communication). The fact that the quadruple and higher collision terms in 3 dimensions diverge has been noted also by Weinstock. See J. Weinstock, Phys. Rev. **132**, 454 (1963).

[2] There is an enormous literature to be cited here. Some of it is given in Refs. 3 and 4 of II.

[3] M. S. Green, International Seminar on the Transport Theory of Gases at Brown University, 1964 (to be published); M. S. Green and R. A. Piccirelli, Phys. Rev. **132**, 1388 (1963).

[4] R. Zwanzig, Phys. Rev. **129**, 486 (1963).

[5] K. Kawasaki and I. Oppenheim, Phys. Rev. **136**, A1519 (1964); **139**, 649 (1965), hereafter referred to as I and II, respectively.

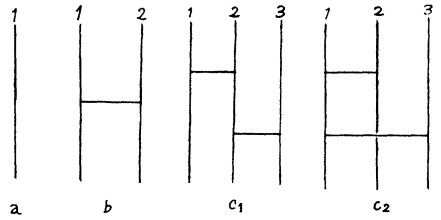


FIG. 1. Diagrams representing $D_0(\epsilon)$, $D_1(\epsilon)$, and $D_2(\epsilon)$.

Since, as we shall see later, in two dimensions the logarithmic divergence appears in the triple-collision term to which the spatial correlation present in the equilibrium configurational-distribution function does not contribute, we shall ignore these spatial correlations. Thus we consider

$$D\equiv\lim_{\epsilon\to 0+}D(\epsilon)\,, \tag{2.2}$$

$$D(\epsilon)\equiv\frac{1}{m^2}\frac{1}{V^N}\int dx^N p_1{}^x G(\epsilon)p_1{}^x\Phi(\mathbf{p}^N)\,, \tag{2.3}$$

where $\Phi(\mathbf{p}^n)$ is the $n$-particle equilibrium momentum space distribution function and $\mathbf{p}^n$ stands for $\mathbf{p}_1, \mathbf{p}_2, \cdots, \mathbf{p}_n$. $x_i$ represents $\mathbf{r}_i$ and $\mathbf{p}_i$.

The first step in obtaining a formal density expansion of (2.3) is to make use of the binary-collision expansion for $G(\epsilon)$:[4]

$$G(\epsilon)=G_0-\sum_\alpha G_0T_\alpha G_0+\sum_\alpha\sum_\beta{}' G_0T_\alpha G_0T_\beta G_0-\cdots\,, \tag{2.4}$$

from which we obtain the corresponding binary-collision expansion of $D(\epsilon)$. If we use the $\mathbf{k}$-vector representation, we obtain

$$D(\epsilon)=D_0(\epsilon)+\rho D_1(\epsilon)+\rho^2D_2(\epsilon)+\rho^2D_3(\epsilon)+\cdots\,, \tag{2.5}$$

where

$$D_0(\epsilon)=\frac{1}{m^2}\int d\mathbf{p}_1\epsilon^{-1}p_1{}^{x^2}\varphi(p_1)\,, \tag{2.6}$$

$$D_1(\epsilon)=\frac{1}{m^2}\int d\mathbf{p}^2p_1{}^x[-\epsilon^{-2}VT_{12}(0|0)]p_1{}^x\Phi(\mathbf{p}^2)\,, \tag{2.7}$$

$$D_2(\epsilon)=\frac{1}{m^2}\int d\mathbf{p}^3p_1{}^x\epsilon^{-3}V^2T_{12}(0|0)\times[T_{13}(0|0)+T_{23}(0|0)]p_1{}^x\Phi(\mathbf{p}^3)\,, \tag{2.8}$$

$$D_3(\epsilon)=\frac{1}{m^2}\int d\mathbf{p}^3p_1{}^x[-\tfrac{1}{2}\epsilon^{-2}V^2(0|\tau(123)|0)]\times p_1{}^x\Phi(\mathbf{p}^3)\,, \tag{2.9}$$

where $T$ is the binary-collision operator defined by I(2.22) and $\tau(123)$ is defined by I(3.31) and represents the triple collision. The remaining terms in Eq. (2.5) contain higher powers of $\rho$ than $\rho^2$.

For the present problem a diagrammatical analysis is convenient. The processes corresponding to $D_0(\epsilon)$, $D_1(\epsilon)$, and $D_2(\epsilon)$ are represented by Figs. 1(a), (b), and (c), respectively; and some of the processes of the triple collision are presented in Fig. 2. Straight vertical lines represent the propagation of freely moving spatially uncorrelated ($\mathbf{k}=0$) particles and wavy vertical lines represent freely moving but spatially correlated ($\mathbf{k}\neq 0$) particles. The horizontal lines connecting two vertical lines represent binary-collision operators between the two particles represented by the vertical lines. Each section of the vertical lines corresponds to the resolvent operators for free particle motion $G_0$ and, if there is no wavy line in this section, gives rise to a factor $G_0(0|0)=\epsilon^{-1}$. Higher order terms in the binary-collision expansion of $D(\epsilon)$ can readily be represented by similar diagrams.

We now classify these diagrams and consider their contributions to $D(\epsilon)$: (1) Disconnected diagrams which can be divided into more than one part in such a way that no two particles belonging to different parts are connected by binary-collision operators, do not contribute to $D(\epsilon)$. This is because these diagrams involve an operator of the form

$$\int dx_idx_jT_{ij}\cdots\,, \tag{2.10}$$

which vanishes. By the same token, any term vanishes in which $T_{ij}$, $(i\neq j\neq 1)$ appears in such a way that no quantity containing $i$ *or* $j$ appears to the left of $T_{ij}$. (2) Consider the diagrams which can be divided into more than one section by horizontal lines between binary-collision operators cutting through vertical straight lines. A typical example is given in Fig. 3 where the cut is represented by a dotted line. Contributions to $D(\epsilon)$ arising from these diagrams are simply the products of operators corresponding to the separate sections with extra factors of $\epsilon^{-1}$. In our method of density expansion, the term with the highest power of $\epsilon^{-1}$ in each order of the binary-collision expansion belonging to this category, such as the one represented by Fig. 1($c_2$), is simply the product of terms represented by Fig. 1(b) [or $\mathfrak{L}(\mathbf{p}_1)$, (2.18), below], and does not appear in the inverted series. As far as the first density correction to transport coefficients is concerned, the terms with lower powers of $\epsilon^{-1}$ belonging to this category such as the one represented by Fig. 1($c_1$) are combined with

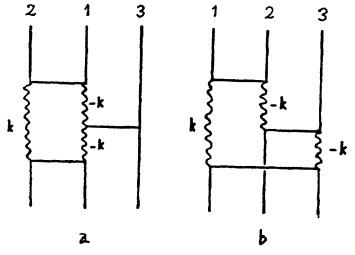


FIG. 2. A part of the triple-collision process which diverges in two dimensions. Another divergent contribution is given by interchanging 1 and 2 in Fig. 2(a).

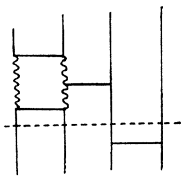

FIG. 3. A diagram belonging to the category (2).

the terms arising from spatial correlations in the equilibrium distribution function to produce a finite contribution to the first density correction. This is discussed in I in detail for the case of shear viscosity. Therefore, we need not consider the terms belonging to this category. (3) Thus, the diagrams we must consider consist of those connected diagrams which cannot be separated into more than one part by horizontal cuts through the particle lines with $\mathbf{k}=0$. Typical diagrams of this category are shown in Fig. 1(b) which contributes to the lowest order term in the density expansion of $D(0+)$ and the triple-collision diagrams represented by Fig. 2 which contribute to the finite first density correction to $D$ in 3-dimensional systems.

Let us now rewrite $D_3(\epsilon)$ as follows:

$$D_3(\epsilon)=-\frac{1}{\epsilon^2}\frac{1}{m^2}\int d\mathbf{p}_1 p_1{}^x t(\mathbf{p}_1) p_1{}^x \varphi(p_1), \quad (2.11)$$

where

$$t(\mathbf{p}_1)\equiv t_D(\mathbf{p}_1)+t_C(\mathbf{p}_1), \quad (2.12)$$

$$t_D(\mathbf{p}_1)\equiv \int\int d\mathbf{p}_2 d\mathbf{p}_3 V^2(0|[T_{12}G_0T_{13}G_0T_{12}+T_{12}G_0T_{23}G_0T_{12} +T_{12}G_0T_{23}G_0T_{13}]|0)\varphi(p_2)\varphi(p_3), \quad (2.13)$$

$$t_C(\mathbf{p}_1)\equiv \int\int d\mathbf{p}_2 d\mathbf{p}_3 V^2(0|[T_{12}G_0T_{13}G_0T_{23} -\tfrac{1}{2}\{\sum{}' T_\alpha G_0 T_\beta G_0 T_\gamma G_0 T_\delta - \cdots\}]|0) \times\varphi(p_2)\varphi(p_3). \quad (2.14)$$

The summation in (2.14) is taken over all possible pairs of particles 1, 2 and 3 excluding consecutive appearances of the same pair, and the dots indicate higher terms in the binary-collision expansion of the triple collision operator $t$.

Zwanzig's technique[4] of inverting the series (2.5) then yields the following expression for the formal density expansion of $D$:

$$D=\rho^{-1}D^{(0)}+D^{(1)}+\cdots, \quad (2.15)$$

$$D^{(0)}\equiv\frac{1}{m^2}\int d\mathbf{p}_1 p_1{}^x \mathfrak{L}_+{}^{-1}(\mathbf{p}_1) p_1{}^x \varphi(p_1), \quad (2.16)$$

$$D^{(1)}\equiv-\frac{1}{m^2}\int d\mathbf{p}_1 p_1{}^x \mathfrak{L}_+{}^{-1}(\mathbf{p}_1) \times t_+(\mathbf{p}_1)\mathfrak{L}_+{}^{-1}(\mathbf{p}_1) p_1{}^x \varphi(p_1), \quad (2.17)$$

where

$$\mathfrak{L}(\mathbf{p}_1)\equiv V\int T_{12}(0|0)\varphi(p_2)d\mathbf{p}_2, \quad (2.18)$$

and we attach suffices $+$ to those operators for which the limit $\epsilon\to 0+$ has already been taken. In obtaining this result, we have ignored the term involving $T_{23}$ in (2.8), since it is represented by a diagram of category (2) and contributes to the finite first correction to $D$ as we mentioned earlier, and is of no interest in the present work.

Since the divergences mentioned in Sec. 1 first appear in $t_D(\mathbf{p}_1)$, (2.13), for 2-dimensional systems, we shall consider this term in detail in the following sections.

## 3. DIVERGENCE AND ITS ELIMINATION

We now consider the first term in (2.13) which is represented by Fig. 2(a), namely,

$$t_{Da}(\mathbf{p}_1)\equiv\int\int d\mathbf{p}_2 d\mathbf{p}_3 V^2(0|T_{12}G_0T_{13}G_0T_{12}|0)\varphi(p_2)\varphi(p_3)$$

$$=\frac{1}{(2\pi)^d}\int d\mathbf{k}\int\int d\mathbf{p}_2 d\mathbf{p}_3 V^3 T_{12}(0|\mathbf{k},-\mathbf{k},0) \times g(\mathbf{k},-\mathbf{k},0)T_{13}(\mathbf{k},-\mathbf{k},0|\mathbf{k},-\mathbf{k},0) \times g(\mathbf{k},-\mathbf{k},0)T_{12}(\mathbf{k},-\mathbf{k},0|0)\varphi(p_2)\varphi(p_3), \quad (3.1)$$

where $d$ is the number of dimensions, we have replaced the summation over $\mathbf{k}$ by an integration, and $g(\mathbf{k}^N)$ is the diagonal element of the free-particle resolvent operator $G_0$ given by

$$g(\mathbf{k}^N)=[\epsilon+i\mathbf{k}^N\cdot\mathbf{p}^N/m]^{-1}.$$

Let us now examine the integral over $\mathbf{k}$ in (3.1) in the limit $\epsilon\to 0+$. Since for small $|\mathbf{k}|$ the $T_\alpha$'s are finite and $g(\mathbf{k},-\mathbf{k},0)$ behaves like $1/k$, the integrand in (3.1) goes as $1/k^2$ for small enough values of $k$. In two dimensions, the $\mathbf{k}$ integral shows a logarithmic divergence near $\mathbf{k}=0$ whereas it is finite for 3 dimensions. This is the origin of the divergence found by Cohen, Dorfman, and Sengers. Evidently, the other terms of (2.13) also show the same logarithmic divergence. For 3 dimensions the same kind of divergence begins to appear in the quadruple collisions as one can see by analyzing the typical quadruple collision diagrams of Fig. 4.

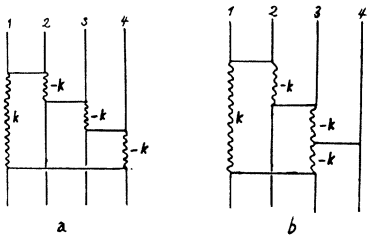


FIG. 4. A part of quadruple collisions which diverges in three dimensions.

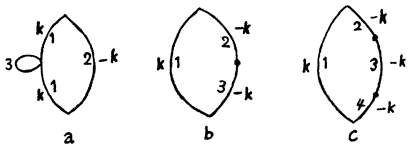

FIG. 5. Ring diagrams corresponding to Fig. 2 and Fig. 4(a).

The first term of (2.14) does not diverge because as far as the divergence is concerned, $T_\alpha$'s can be replaced by $T_\alpha(0|0)$ in the $\mathbf{k}$ representation and

$$T_{23}(0|0)\varphi(p_2)\varphi(p_3)\rightarrow 0 \quad \text{as} \quad \epsilon\rightarrow 0+. \qquad (3.2)$$

It is also clear that the terms involving more than 3 $T$'s in the triple collision operator which occur in the second term of $t_C(\mathbf{p}_1)$ possess no divergences in two dimensions because, for each additional factor of $T$ beyond the third one, we have one factor of $1/k$ and one integration over $\mathbf{k}$.

The fact that the triple-collision operator contains divergences near $\mathbf{k}=0$ or at large distances in two dimensions indicates that the collisions of the three particles with the rest of the system cannot be ignored even in calculating the first density correction to $D$.[6] This reminds us of the familiar situation encountered in dealing with a system of particles interacting with Coulomb potentials where the density expansion shows similar divergences due, in this case, to the long range nature of the Coulomb potential. Such divergences have been eliminated by summing over the most divergent contributions coming from all orders in the density (ring diagrams[7]). We shall investigate whether or not the divergences in our problem can be eliminated by summing over the most divergent higher order terms in the binary-collision expansion (2.4) and (2.5).

Our first task is to find the most divergent terms in each order of the binary-collision expansion, restricting ourselves to the terms belonging to category (3) of Sec. 2. Extending the reasoning for the case of triple collision operators, one easily arrives at the conclusion that the most divergent contributions which have $nT$'s involve $n$ different particles. Considering the restriction defining category (3) of Sec. 2, these terms are characterized by a single $\mathbf{k}$ vector. This can be seen as follows: First let us separate out those particles out of $n$ particles which carry zero wave vectors, such as the particle 4 in Fig. 4(b); and suppose that there are $s$ such particles. For the rest, the number of $T$'s available is clearly the same as the number of the remaining particles, and each particle is connected to the rest by at least two $T$'s. The only possible way of connecting these $n-s$ particles by $n-s$ $T$'s is to form a ring with $n-s$ $T$'s and $n-s$ particles which carry a single wave vector $\mathbf{k}$ as shown in Fig. 4. If we add another $T$ to these terms without increasing the numbers of particles, another ring carrying another wave vector $\mathbf{k}'$ is formed. This will bring about an additional factor of $k'$, thus rendering the contribution less divergent.

Examples given in Fig. 4 show a divergence proportional to $1/k_0$ where $k_0$ is a cutoff wave number at small $k$. The terms involving $n$ particles diverge as $k_0^{-(n-3)}$, $n\geq 4$.

For the subsequent discussion, it is convenient to change the diagrammatic representation in order to have a closer connection with the familiar ring diagrams.[7] Figures 5(a), (b), and (c) represent the ring diagrams corresponding to Figs. 2(a) and (b), and Fig. 4(a), respectively. In Fig. 5(a), the small loop labeled 3 indicates a collision of the particles 1 and 3 without a transfer of the $\mathbf{k}$ vector. The dot in Fig. 5(b) designates the collision of the particle pair 23 where the $\mathbf{k}$ vector is transferred from the particle 2 to the particle 3. The first and the last binary collisions in each term are represented by the two cusps at the top and the bottom of the corresponding ring, respectively. Now, again as far as the divergences are concerned, the $T_\alpha$'s in the most divergent terms can be replaced by $T_\alpha(0|0)$ in the $\mathbf{k}$ representation. Thus, the first and the last $T_\alpha$'s in each term must involve the particle 1 because of (2.10) and (3.2). Then the most general diagram is the ring with two cusps decorated with an arbitrary number of loops attached to the arc labeled 1 and an arbitrary number of loops and dots attached to the other half of the ring starting with particle 2 in an arbitrary order, excluding the diagram with neither loop nor dot. Typical most divergent diagrams are given in Figs. 5 and 6 where the left and right halves of the ring carry the wave vectors $\mathbf{k}$ and $-\mathbf{k}$, respectively. Figure 6(a) represents the following sequence of processes: (1) a collision between the particles 1 and 2 creating the wave vectors $\mathbf{k}$ and $-\mathbf{k}$; (2) the collision of 1 with 3 without the transfer of the $\mathbf{k}$ vector; (3) the collision of 2 with 4 without the transfer of the $\mathbf{k}$ vector; (4) the collision of 1 with 5 without the transfer of the $\mathbf{k}$ vector; (5) the collision of 2 with 6 with the transfer of $-\mathbf{k}$ from 2 to 6; (6) the collision of 1 and 6 annihilating the $\mathbf{k}$ vector created in the process (1). Figure 6(b) can be interpreted in a similar manner. Here we have omitted the class of diagrams represented by Fig. 7 in which the particle 2 which has interacted with another particle before interacts with still another particle (4 in Fig. 7) while it carries no $\mathbf{k}$ vector. This particle cannot coincide with

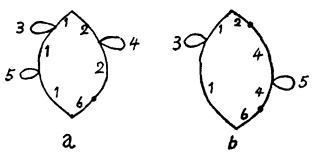

FIG. 6. More complex ring diagrams.

[6] Here we define the triple collision in such a way that in the diagram representing the triple collision no free-particle propagator with $\mathbf{k}=0$ appears (see Fig. 2). This definition may not be the same as other definitions; for instance, the one in which during the collision process any particle is within the force range of at least one of the other two particles.

[7] M. Gell-Mann and K. A. Brueckner, Phys. Rev. **106**, 364 (1957); R. Balescu, Phys. Fluids **3**, 52 (1960). The precise meaning of the present diagrams is, however, different from those used in these references.

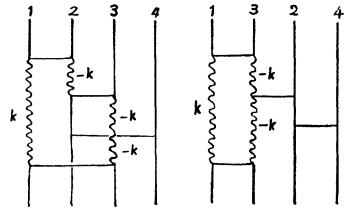


FIG. 7. Less divergent diagrams.

the particle 1 since the particle 1 always carries the $\mathbf{k}$ vector during the whole event. The terms corresponding to these diagrams can be shown not to be the most divergent ones by the same argument as before which uses (3.2). Summing up all the most divergent contributions, $t_D(\mathbf{p}_1)$, (2.13), is modified to become another operator here denoted by $\tilde{t}(\mathbf{p}_1)$.

Succinct expressions for general terms in this expansion can be obtained by introducing the two operators $\Lambda_l$ and $\Lambda_d$ corresponding to a loop and a dot, respectively, which can operate on another operator. If a line labelled, say, 1 enters a loop or a dot from above, these operators are defined by,

$$\Lambda_l(1)A \equiv \int VT_{13}G_0 A\,\varphi(p_3)d\mathbf{p}_3, \tag{3.3}$$

$$\Lambda_d(1)A \equiv \int VT_{13}G_0\mathcal{P}_{13}A\,\varphi(p_3)d\mathbf{p}_3, \tag{3.4}$$

respectively, where $A$ is an arbitrary operator containing the variable $x_1$ and $\mathcal{P}_{13}$ is a particle-exchange operator which does not act on $\varphi(p_i)$. Then one can immediately write down contributions to $\tilde{t}(\mathbf{p}_1)$ arising from Figs. 5(a), (b), and (c) as follows:

$$\tilde{t}_a(\mathbf{p}_1) = \int V(0|T_{12}G_0\Lambda_l(1)T_{12}|0)\varphi(p_2)d\mathbf{p}_2, \tag{3.5}$$

$$\tilde{t}_b(\mathbf{p}_1) = \int V(0|T_{12}G_0\Lambda_d(2)T_{12}|0)\varphi(p_2)d\mathbf{p}_2, \tag{3.6}$$

$$\tilde{t}_c(\mathbf{p}_1) = -\rho\int V(0|T_{12}G_0\Lambda_d(2)\Lambda_d(2)T_{12}|0) \times\varphi(p_2)d\mathbf{p}_2, \tag{3.7}$$

where the factor $\rho$ in (3.7) comes from the $N-3(\cong N$ as $N\to\infty)$ possible choices of the particle 4.

Generalizations to more complex ring diagrams are obvious. For each additional loop attached to the left half of the ring, and loop or dot attached to the right half we add a factor $\Lambda_l(1)$ and a factor $\Lambda_l(2)$ or $\Lambda_d(2)$, respectively, the order of the factors being determined by that of the corresponding loops or dots in the diagram. (Loops and dots are ordered in any diagram in a definite way from the top to the bottom irrespective of which half of the ring they are attached to.) Thus, the summation of all the contributions yields

$$\tilde{t}(\mathbf{p}_1) = \int V(0|T_{12}G_0\sum_{n=1}^{\infty}\sum_{\{u_i\}}\sum_{\{\alpha_i\}}(-\rho)^{n-1}\Lambda_{u_1}(\alpha_1) \times\Lambda_{u_2}(\alpha_2)\cdots\Lambda_{u_n}(\alpha_n)T_{12}|0)\varphi(p_2)d\mathbf{p}_2, \tag{3.8}$$

where

$$u_i = l \quad \text{if} \quad \alpha_i = 1, \quad u_i = l \text{ or } d \quad \text{if} \quad \alpha_i = 2.$$

This can be simplified as

$$\tilde{t}(\mathbf{p}_1) = \int V(0|T_{12}G_0\Lambda(12) \times[1+\rho\Lambda(12)]^{-1}T_{12}|0)\varphi(p_2)d\mathbf{p}_2, \tag{3.9}$$

where

$$\Lambda(12) \equiv \Lambda_l(1)+\Lambda_l(2)+\Lambda_d(2). \tag{3.10}$$

If we compare (3.9) with (2.13) which is written as

$$t_D(\mathbf{p}_1) = \int V(0|T_{12}G_0\Lambda(12)T_{12}|0)\varphi(p_2)d\mathbf{p}_2, \tag{3.11}$$

we see that (3.9) contains an extra factor $[1+\rho\Lambda(12)]^{-1}$. This extra factor provides a natural cutoff at small $k$ of the divergent integral (3.11). First let us write (3.9) in the $\mathbf{k}$ representation as follows:

$$\tilde{t}(\mathbf{p}_1) = \frac{1}{(2\pi)^2}\int d\mathbf{k}\int d\mathbf{p}_2 VT_{12}(0|\mathbf{k},-\mathbf{k})g(\mathbf{k},-\mathbf{k})\Lambda(\mathbf{k},-\mathbf{k}) \times[1+\rho\Lambda(\mathbf{k},-\mathbf{k})]^{-1}T_{12}(\mathbf{k},-\mathbf{k}|0)\varphi(p_2), \tag{3.12}$$

where

$$\Lambda(\mathbf{k},-\mathbf{k}) \equiv \Lambda_l^{(\mathbf{k})}(\mathbf{p}_1)+\Lambda_l^{(-\mathbf{k})}(\mathbf{p}_2)+\Lambda_d^{(-\mathbf{k})}(\mathbf{p}_2), \tag{3.13}$$

with

$$\Lambda_l^{(\mathbf{k})}(\mathbf{p}_1) \equiv \int VT_{13}(\mathbf{k},-\mathbf{k},0|\mathbf{k},-\mathbf{k},0) \times\left[\epsilon+i\frac{\mathbf{p}_1-\mathbf{p}_2}{m}\cdot\mathbf{k}\right]^{-1}\varphi(p_3)d\mathbf{p}_3, \tag{3.14}$$

$$\Lambda_d^{(-\mathbf{k})}(\mathbf{p}_2) \equiv \int VT_{23}(\mathbf{k},-\mathbf{k},0|\mathbf{k},0,-\mathbf{k}) \times\left[\epsilon+i\frac{\mathbf{p}_1-\mathbf{p}_3}{m}\cdot\mathbf{k}\right]^{-1}\mathcal{P}_{23}\varphi(p_3)d\mathbf{p}_3, \tag{3.15}$$

and $\Lambda_l^{(\mathbf{k})}(\mathbf{p}_2)$ is obtained from (3.14) by replacing $\mathbf{p}_1$ by $\mathbf{p}_2$.

As $\mathbf{k}$ approaches zero, $g(\mathbf{k},-\mathbf{k})$ as well as $\Lambda(\mathbf{k},-\mathbf{k})$ behaves as $1/k$ in the limit $\epsilon\to 0+$, and $[1+\rho\Lambda(\mathbf{k},-\mathbf{k})]^{-1}$ provides a factor $k$, eliminating the logarithmic divergence. The magnitude of the cutoff wave vector $k_0$ which is the magnitude of $k$ when $\rho\Lambda(\mathbf{k},-\mathbf{k})$ becomes of the order of 1 can be estimated by noting that for

small $k$,

$$VT_{13}(\mathbf{k},-\mathbf{k},0|\mathbf{k},-\mathbf{k},0)$$
$$\cong VT_{13}(\mathbf{k},-\mathbf{k},0|0,-\mathbf{k},\mathbf{k})\cong VT_{13}(0|0)\sim v\sigma, \quad (3.16)$$

where $v$ is the average velocity of the particles and $\sigma$ is the collision cross section. Then from (3.14) and (3.15)

$$\Lambda(\mathbf{k},-\mathbf{k})\sim\sigma/k \quad (3.17)$$

for small $k$. Thus, we estimate that

$$k_0\sim\rho\sigma\sim(\text{mean free path})^{-1}, \quad (3.18)$$

and the guess[1] as to the magnitude of the cutoff is justified. Since (3.12) is logarithmically divergent at small $k$ in the absence of the factor $[1+\rho\Lambda(\mathbf{k},-\mathbf{k})]^{-1}$ and this factor gives a cutoff given by (3.18), it is now clear that $\tilde{l}(\mathbf{p}_1)$ contains a term $\ln\rho$, and thus the self-diffusion coefficient $\mathbf{D}$ has the form

$$\mathbf{D}=A\rho^{-1}+B\ln\rho+C+\cdots, \quad (3.19)$$

where $A, B, C, \cdots$ depend only on the temperature. The term $A\rho^{-1}$ is the low density limit of Chapman and Enskog, (2.16). The term $B$ is determined by the coefficient of $\ln k_0$ of the logarithmically divergent term $t_D(\mathbf{p}_1)$ in the absence of the cutoff by using (2.17). In order to determine $C$, we need the complete analysis of the most divergent contributions as given in this section. This situation is the same as in the case of the electron gas[7]; namely, $\tilde{l}(\mathbf{p}_1)$ gives rise to a density independent contribution in addition to the $\ln\rho$ term plus a part of the higher density corrections. This together with the density-independent contributions coming from $t_C(\mathbf{p}_1)$ and from the spatial correlation in the equilibrium configurational distribution function which we have ignored up to now constitute $C$.

## 4. CONCLUDING REMARKS

The logarithmic divergence in the triple-collision term in the density expansion of the transport coefficients in two dimensions recently discovered by Cohen, Dorfman, and Sengers has been eliminated by summing over the most divergent contributions coming from all orders of the binary-collision expansion of the resolvent operator appearing in the correlation function expression for the transport coefficients. A detailed analysis has been presented for the case of the self-diffusion coefficient, and its density expansion is obtained in the form (3.19).

A similar analysis for the shear viscosity and the thermal conductivity should yield density expansions of the form

$$A+B\rho\ln\rho+C\rho+\cdots, \quad (4.1)$$

In 3 dimensions the divergence first appears in quadruple collisions and the form of the transport coefficients is

$$A+B\rho+C\rho^2\ln\rho+D\rho^2+\cdots. \quad (4.2)$$

Although the transport coefficients are no longer analytic functions of the density, the first density corrections to them are still valid. The expressions for them obtained earlier are still valid, although the assumptions used in deriving them are no longer justified. Nevertheless the present work shows that we can still obtain a systematic density expansion of the transport coefficients by suitably extending the resolvent operator technique for calculating the autocorrelation-function expressions of Zwanzig and the authors.

*Note added in proof.* After submitting this paper, we have learned that the same kind of divergence has been found and discussed by Goldman and Frieman [R. Goldman and E. A. Frieman, Bull. Am. Phys. Soc. **10**, 531 (1965) and private communication].

Diagrams similar to our Figs. 1–4 and 7 have also been used by Fujita in a similar context. [S. Fujita, Introduction to Non-Equilibrium Quantum Statistical Mechanics (to be published)].

## ACKNOWLEDGMENTS

We would like to thank Dr. J. V. Sengers for the very stimulating conversations which provided the motivation for the present work.